Paper No.
62—WA-164

Fatigue Characteristics of Open-End Thick-Walled Cylinders Under Cyclic Internal Pressure

T. E. DAVIDSON
Chief, Physical and Mechanical Metallurgy Laboratory, Watervliet Arsenal, Watervliet, N. Y.

R. EISENSTADT
Associate Professor, Mechanical Engineering Department, Union College, Schenectady, N. Y.

A. N. REINER
Mechanical Engineer, Physical and Mechanical Metallurgy Laboratory, Watervliet Arsenal, Watervliet, N. Y.

Thick-walled cylinder fatigue data due to cyclic internal pressure for open-end cylinders in the range of 10^3 to 10^5 cycles to failure and having a diameter ratio of 1.4 to 2.0 at a nominal yield strength of 160,000 pounds per square inch is presented. Discussed and also presented are the effects of autofrettage on the fatigue characteristics of thick-walled cylinders. Autofrettage substantially enhances fatigue characteristics at stress levels below the corresponding overstrain pressure, the degree of improvement increasing the decreasing stress levels. The rate of improvement in fatigue characteristics increases significantly with diameter ratio in autofrettaged cylinders up to a diameter ratio of 1.8–2.0 and to a much smaller degree in the nonautofrettaged condition. The rate of improvement of fatigue characteristics above 2.0 is the same for both the autofrettaged and nonautofrettaged cases.

It is shown that thermal treatment of 675 F for 6 hours after autofrettage does not affect fatigue characteristics and that there is a correlation between the cyclic-stress level and the area and depth of the fatigue crack to the point of ductile rupture. The depth of the fatigue crack decreases with increasing cyclic-stress level.

A means for using data from a unidirectional tensile fatigue test to predict the fatigue characteristics of thick-walled cylinders is discussed.

Introduction

THE current trend is toward the design of pressure vessels for use at higher operating stress levels. One of the most common techniques for extending the elastic load-carrying capacity is by autofrettage. For example, the operating pressure-to-weight ratio for cannon-type weapons has been substantially increased in recent years by the combined use of high-strength materials and autofrettage. Similar advances have been made in other areas where the requirement exists for vessels capable of operating at very high pressures.

In many instances, the operation of highly stressed pressure vessels is cyclic in nature. In these instances, it is not enough to consider the yielding characteristics alone, but one must also take into account the problem of fatigue life and the manner in which it is affected by such techniques as autofrettage for increasing elastic load-carrying capacity. This report summarizes the results of an experimental program aimed at the study of the fatigue characteristics of high-strength open-end cylinders of intermediate diameter ratio.

The fatigue characteristics of a closed-end cylinder cyclically stressed in the region of the endurance limit have been reported by Morrison, et al. [1].[1] He has found that, in the region of the endurance limit, the residual stresses associated with overstrain substantially enhance fatigue life. Similar results were found by Newhall and Kosting [2] for several rifled sections of cannon tubes, at somewhat higher stress levels.

In light of the current interest in the use of highly stressed pressure vessels, the investigation to be described herein involves a study of fatigue characteristics of thick-walled cylinders in what is commonly referred to as the low-cycle fatigue range, that is up to approximately 10^5 cycles to failure. Presented are data for open-end cylinders in the diameter-ratio range of 1.4 to 2.0 at a nominal yield-strength level of 160,000 pounds per square inch. Data are also presented on the effects of autofrettage on fatigue characteristics as a function of diameter ratio and cyclic stress level. The possibility of utilizing a simple tensile fatigue test to

Contributed by the Metals Engineering Division for presentation at the Winter Annual Meeting, New York, N. Y., November 25–30, 1962, of THE AMERICAN SOCIETY OF MECHANICAL ENGINEERS. Manuscript received at ASME Headquarters, August 6, 1962. Paper No. 62—WA-164.

[1] Numbers in brackets designate References at end of paper.

Nomenclature

σ = stress, pounds per square inch
YS = yield strength, pounds per square inch
UTS = ultimate tensile strength, pounds per square inch
E = modulus of elasticity, pounds per square inch
ν = Poisson's ratio
P = test pressure, pounds per square inch
b = outside diameter of cylinder, in.
a = inside diameter of cylinder, in.
W = wall ratio b/a
NA = nonautofrettaged
A = autofrettaged
D = ratio of lower limit of a confidence level to least-squares value
N = cycles to failure
R = radius of elastic-plastic interface, in.
t = confidence-level coefficient
S = standard deviation
x = logarithm to base 10 of cycles to failure
n = number of experimental points
d = depth of crack, in.
r = correlation coefficient
w = wall thickness, in.

Subscripts

$(\ )_t$ = tangential
$(\ )_r$ = radial
$(\ )_z$ = longitudinal
$(\ )_y$ = yield
$(\ )_p$ = plastic
$(\ )_{trp}$ = tangential residual plastic
$(\ )_{rrp}$ = radial residual plastic
$(\ )_c$ = confidence level
$(\bar{\ })$ = least squares value of function

predict the life of thick-walled cylinders, and the mode of fatigue fracture for cylinders exposed to cyclic internal pressures is discussed.

Procedure

Test Specimens. The specimens utilized in this program consisted of a common one-inch internal diameter and diameter ratios of 1.4, 1.6, 1.8, and 2.0.

The specimen material was of a 4340-type composition with the following nominal chemical analysis in percent:

Carbon	0.37	Nickel	2.39
Manganese	0.72	Chromium	0.98
Silicon	0.28	Molybdenum	0.38
Sulfur	0.035	Phosphorus	0.016

Specimens were heat-treated to a nominal yield strength of 160,000 pounds per square inch by austenizing at 1525 F, oil quenching, and tempering at 1075 F ± 25 deg. Tensile and Charpy test specimens were taken from each group of three specimens which were heat-treated in 40-inch lengths.

After heat-treatment, sufficient material was removed from the bore to eliminate any decarburization. The final surface finish on the internal diameter ranged from 16 to 125 RMS.

The autofrettaged specimens were overstrained 100 percent in the manner described in reference [3]. Those specimens that were thermally treated after autofrettage to reduce anelastic effects were subjected to a temperature of 675 F for 6 hours.

Test Apparatus. The pressure systems used in this program consisted of two basic types. The first is a Harwood Engineering Company System of 80,000 pounds per square inch capacity with a cyclic rate of up to 20 cycles/minute. As shown in the background of Fig. 1, the pressure source consists of an intensifier-type pump which feeds high-pressure fluid into the specimens through a manifold. As can be noted from the figure, four specimens may be tested simultaneously. The holding press serves to support the pressure packings which effectively eliminates longitudinal forces in the specimen, thus resulting in the open-end condition for the specimens. Upon attaining the peak pressure, a valve is opened and the pressure dropped to near atmospheric level. The high-pressure fluid is an instrument oil. A schematic of this system is shown in Fig. 2.

The second type is a Harwood Engineering Company System of 150,000 pounds per square inch capacity with a cyclic rate of up to 10 cycles/minute and consists of an intensifier-type pumping system which feeds pressure into the specimens. In contrast to the former system, the pressure is released by removing the drive pressure in the intensifier instead of venting to atmosphere: thus resulting in a closed system. This results in the pressure not returning to zero between cycles, but to a value of approximately 2500 pounds per square inch. However, since this system is used primarily above 80,000 pounds per square inch, a small residual pressure will have little effect, and the comparative results from both systems are in the range of anticipated experimental error.

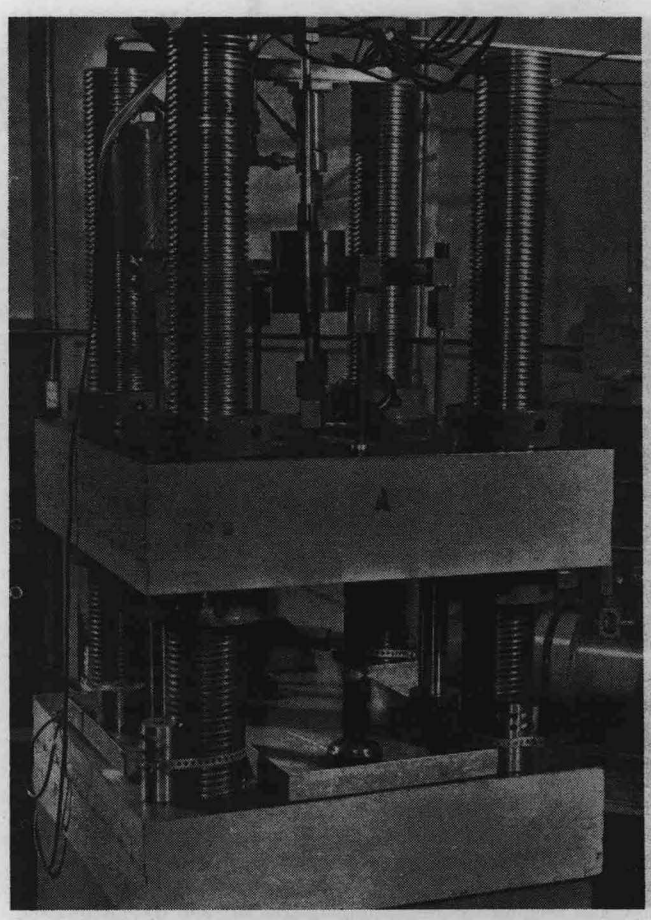

Fig. 1 Holding press and specimens for 80,000 pounds per square inch fatigue system

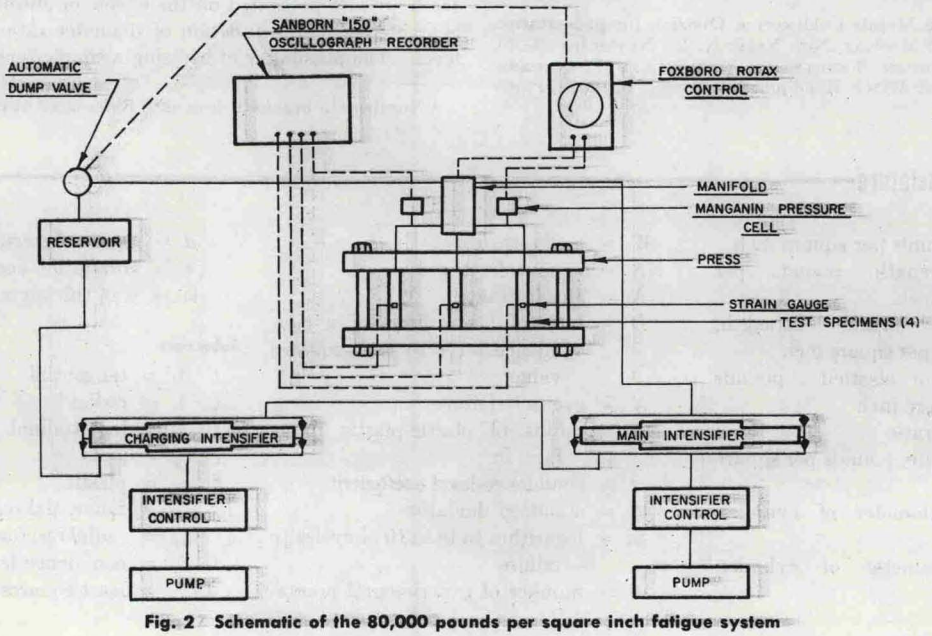

Fig. 2 Schematic of the 80,000 pounds per square inch fatigue system

Instrumentation. 1 **Pressure Control and Recording.** In the 80,000 pounds per square inch system, pressure measurement is by means of Manganin wire-type pressure transducers. Two such transducers are used. One serves as input to the "Rotax" control unit which regulates the automatic cycling of the pressure system through a self-balancing "servo" system equipped with electrical contacts and recording pen. The setting of control contacts relative to the desired indicated pressure determines the point of opening and closing of the dump valve as well as stopping the main intensifier at the end of each pressure peak. The second transducer is used to monitor and record the total pressure cycle on an oscillographic recorder.

The second basic type of pressure transducer, known as a bulk modulus cell, is used in the 150,000 pounds per square inch system. It is a mechanical device designed to sense the linear motion produced by a cylinder with one end closed and exposed to the pressure being measured. This particular system uses a low pressure air transmitter and receiver unit to remotely record and control peak and minimum specimen pressure.

The error in the measurement and recording of pressure is estimated to be approximately one percent in the calibration of the pressure transducer and two percent in the recording system due to the cyclic conditions.

2 **Strain Measurement and Recording.** To insure that each specimen is at the anticipated test pressure, two strain gauges are mounted diametrically opposite each other at the mid-length of each specimen. The output of one gauge on each specimen is monitored on an oscillographic recorder. In normal operation the instruments are set to record the full elastic strain cycle.

Theory

Fatigue failure can be divided into two phases. The first phase consists of the microscopic initiation of the crack. The second stage consists of the propagation of the fatigue crack to the point where the specimen or component can no longer support the applied cyclic load and failure occurs. To a great extent, this second stage is dependent upon the applied tensile stress and, therefore, would be affected by superimposed mean or residual stresses and stress gradients. It is this second stage that will be of primary concern in this paper.

It is well known that a compressive mean stress increases the allowable cyclic-stress amplitude for a given fatigue life. Conversely, a mean tensile stress decreases the allowable amplitude stress as shown qualitatively in Fig. 3, the fatigue strength diagram from H. Sigwart [4] where σ_m is the mean and σ the cyclic stress.

In an overstrained thick-walled cylinder, the tangential and radial residual-stress distribution is described by the relationships [3] based on the Tresca yield criterion:

$$\sigma_{trp} = \frac{\sigma_y}{2}\left[\frac{b^2 + R^2}{b^2} + 2\log\frac{r}{R} - \frac{a^2}{b^2 - a^2}\left(\frac{b^2 - R^2}{b^2} + 2\log\frac{R}{a}\right)\left(1 + \frac{b^2}{r^2}\right)\right] \quad (1)$$

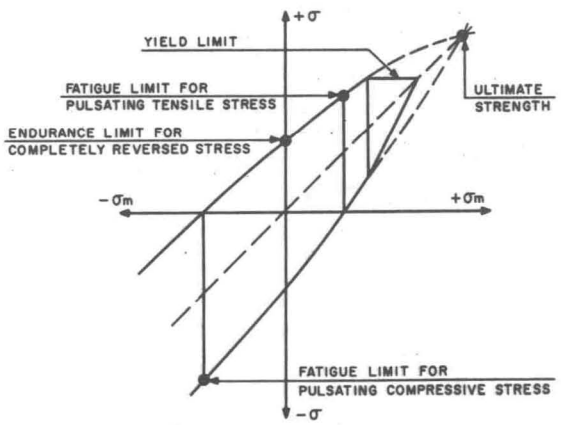

Fig. 3 Fatigue strength diagram

and

$$\sigma_{rrp} = \frac{\sigma_y}{2}\left[\frac{b^2 - R^2}{b^2} + 2\log\frac{r}{R} - \frac{a^2}{b^2 - a^2}\left(\frac{b^2 - R^2}{b^2} + 2\log\frac{R}{a}\right)\left(1 - \frac{b^2}{r^2}\right)\right] \quad (2)$$

For the 100 percent overstrain condition, i.e., $R = b$, these relationships become:

$$\sigma_{trp} = \frac{\sigma_y}{2}\left[2 + 2\log\frac{r}{b} - \frac{a^2}{b^2 - a^2}\left(2\log\frac{b}{a}\right)\left(1 + \frac{b^2}{r^2}\right)\right] \quad (3)$$

and

$$\sigma_{rrp} = \frac{\sigma_y}{2}\left[2\log\frac{r}{b} - \frac{a^2}{b^2 - a^2}\left(2\log\frac{b}{a}\right)\left(1 - \frac{b^2}{r^2}\right)\right] \quad (4)$$

Equations (3) and (4) are shown in Fig. 4 for a 2.0-diameter ratio in the 100 percent overstrain condition. As can be seen, the tangential residual stress is compressive at the bore.

In view of the compressive residual stress, it would be expected that the overstrained, or autofrettaged, cylinder will withstand a higher cyclic pressure for a given life or a longer life for a given stress level than the nonautofrettaged cylinder. Since, for the 100 percent overstrain condition, the magnitude of the residual stresses increases with diameter ratio, it would also be expected that the increased life due to autofrettage would also increase with diameter ratio.

By equating the tangential residual stress to the yield strength of the material in compression, it is found for the 100 percent overstrain condition, assuming the simplified maximum shear-stress yield criterion, that beyond a diameter ratio of approximately 2.2, the cylinder will reverse yield upon the release of the overstrain pressure. Theoretically then, the increase in fatigue characteristics due to autofrettage will approach a maximum at the 2.2-diameter ratio level. As will be shown, however, due to what appears to be the Bauschinger effect, this critical diameter ratio appears to be in the range of 1.8–2.0 instead of 2.2.

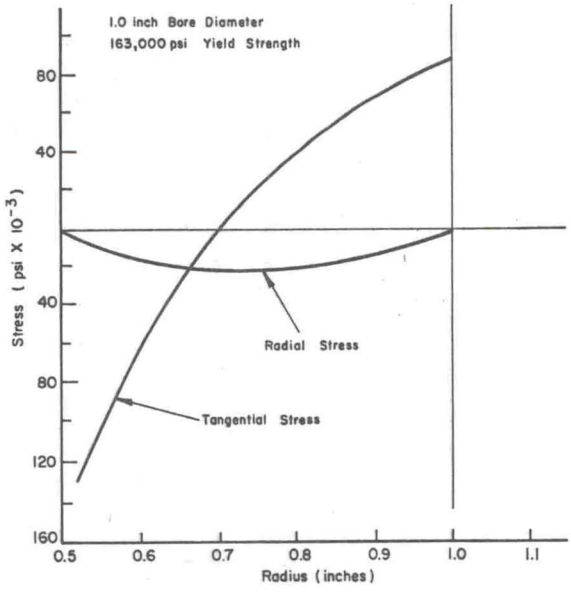

Fig. 4 Residual stress distribution for a 2.0-diameter ratio, 100 percent overstrained cylinder

Results and Discussion

Analysis of Various Cyclic Parameters for Use in Presenting Fatigue Data. In the presentation of fatigue data for thick-walled cylinders, several cyclic parameters may be plotted against life in terms of cycles to failure. How the fatigue data for the non-autofrettaged cylinders appear when plotted in terms of various cyclic parameters is shown in Figs. 5 through 8. For simplicity in comparing the various cyclic parameters, only the least-squares line for each diameter ratio corresponding to the regression of the cycles to failure on the pressure or stress level, along with the correlation coefficient, equation (6), for all of the data in terms of the pertinent cyclic parameter, will be shown in this series of figures.

Based on conventional statistical theory, the general relationship describing the least-squares line for the regression of x on y is:

$$x = a + b(y - \bar{y}) \tag{5}$$

where for the purposes of this investigation

$$y = \log (\text{cyclic parameter})$$

$$a = \bar{y} = \frac{\Sigma y}{n}$$

$$\bar{x} = \frac{\Sigma x}{n} = \frac{\Sigma \log (\text{no. cycles to failure})}{n} \text{ and}$$

$$b = \frac{\Sigma(x - \bar{x})(y - \bar{y})}{\Sigma(y - \bar{y})^2}$$

The correlation coefficient (r) is defined by

$$r = \frac{\Sigma(x - \bar{x})(y - \bar{y})}{\sqrt{\Sigma(x - \bar{x})^2(y - \bar{y})^2}} \tag{6}$$

and is a measure of the effectiveness or probability of the data being described by the defined least-squares line and, as will be shown, is an indication of the relative data spread for the various cyclic parameters.

The data could also be statistically analyzed in terms of the regression of y on x. However, because of the high correlation coefficients of the experimental results, varying from 0.91 to 0.986, there are only minor variations between the regressions, and only one will be shown.

For the purpose of minimizing the effects of minor property variations in the test specimens, and to enable comparison of the results of this work with those of other investigators, all cyclic parameters and the data presented herein will be normalized with

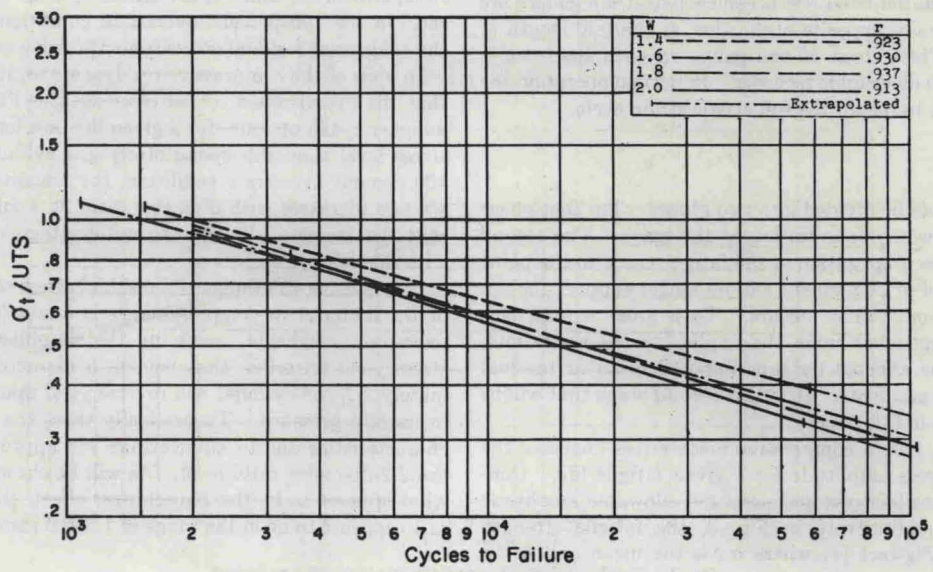

Fig. 5 Tangential bore stress versus cycles to failure

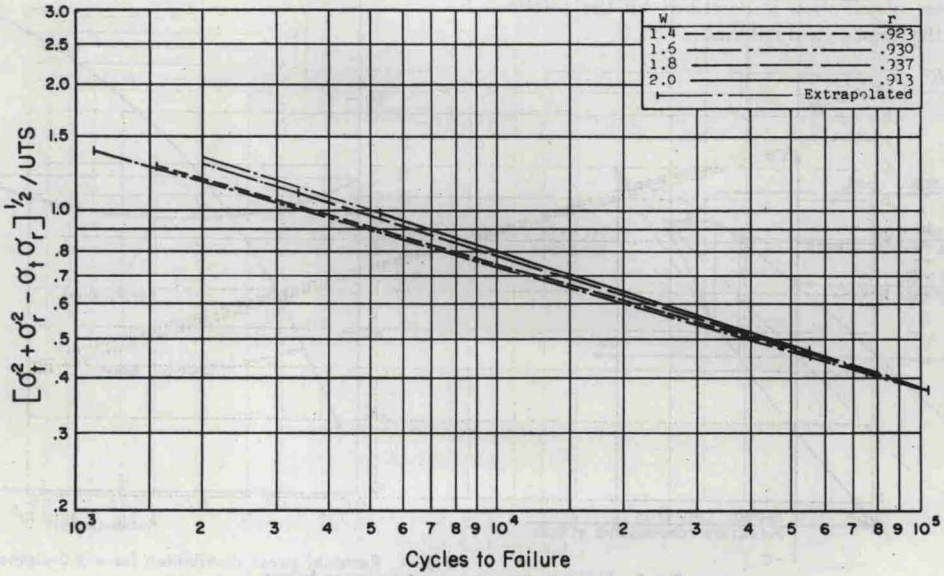

Fig. 6 Difference in principal bore stress versus cycles to failure

respect to the ultimate tensile strength, except where otherwise specified.

In the simplest form, the data may be plotted as cyclic pressure versus cycles to failure. Because a summary curve utilizing this parameter will be subsequently shown, it is sufficient to say, that, since the tangential stress is proportional to diameter ratio, the curve will consist of a series of widely separated lines corresponding to each diameter ratio.

Fig. 5 shows normalized maximum tangential stress at the bore which is defined as

$$\frac{\sigma_t}{\text{UTS}} = \frac{P}{\text{UTS}} \frac{W^2 + 1}{W^2 - 1} \tag{7}$$

as a function of cycles to failure. As would be expected, a large amount of the diameter-ratio dependence has been removed. It should be noted, however, that the least-squares line for the smaller diameter ratio is at a higher value than the larger diameter ratio. This is opposite to what would be expected. The actual initiation of the fatigue crack can probably be predicted by some cyclic stress or strain parameter independent of diameter ratio. The crack, however, must propagate over a larger area in the larger diameter. Intuitively then, the larger diameter ratio should be at a higher stress and life level. Based on this, fatigue failure is probably some function of a combined stress condition instead of a single principal stress.

Fig. 6 shows the difference in the principal stresses at the bore as defined by

$$\frac{\sigma_t - \sigma_r}{\text{UTS}} = \frac{2PW^2}{\text{UTS}(W^2 - 1)} \tag{8}$$

as a function of the number of cycles to failure. As can be noted, the diameter-ratio dependency is small with the larger diameter ratio logically exhibiting the higher fatigue-strength characteristics.

Fig. 7 shows the data in terms of the normalized octahedral stress as defined by

$$\frac{1}{\text{UTS}} \left\{ [(\sigma_t - \sigma_r)^2 + (\sigma_r - \sigma_z)^2 + (\sigma_z - \sigma_t)^2] \frac{1}{2} \right\}^{1/2} \tag{9}$$

which, since $\sigma_z = 0$, yields

$$\frac{1}{\text{UTS}} [\sigma_t^2 + \sigma_r^2 - \sigma_t \sigma_r]^{1/2} \tag{10}$$

A strain parameter defined by

$$\frac{\sigma_t - \nu\sigma_r}{E} \tag{11}$$

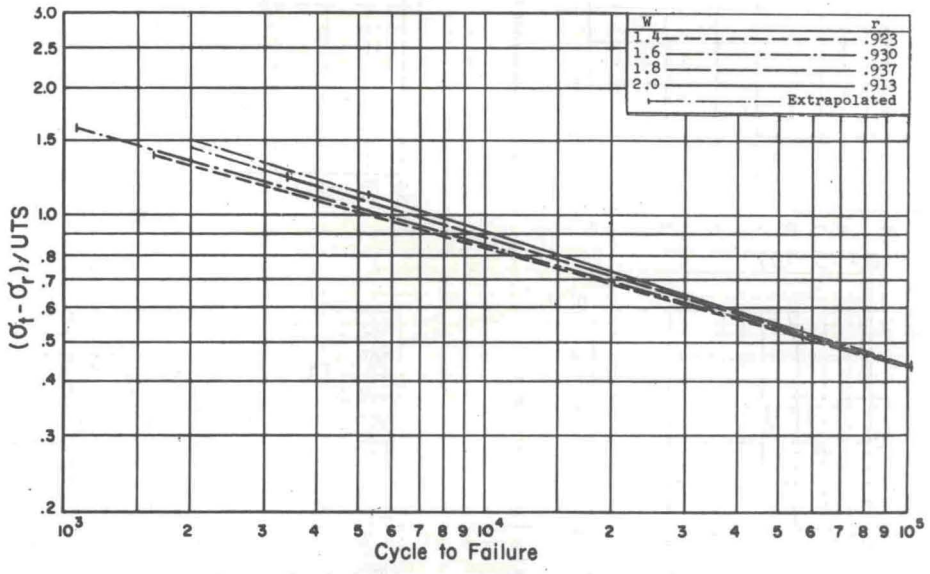

Fig. 7 Octahedral stress parameter versus cycles to failure

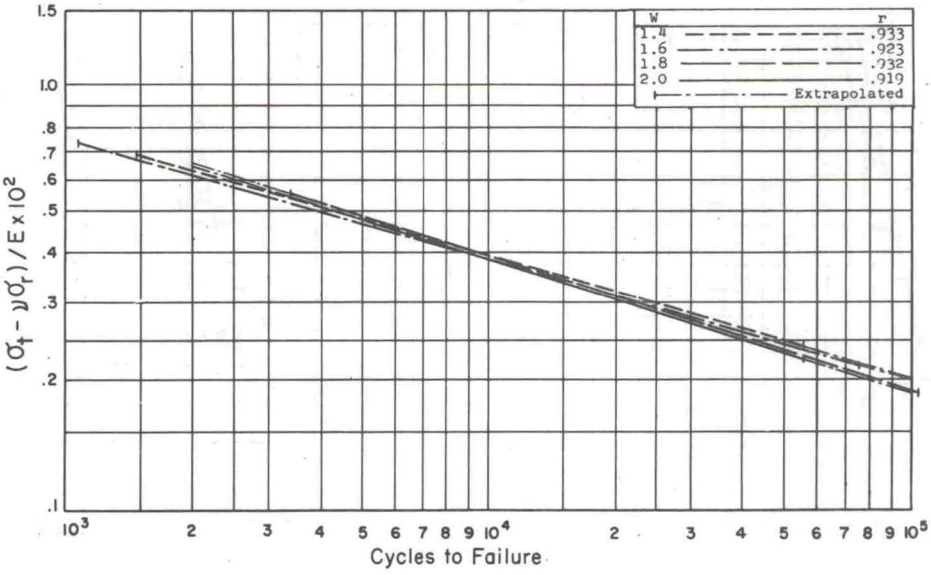

Fig. 8 Strain parameter versus cycles to failure

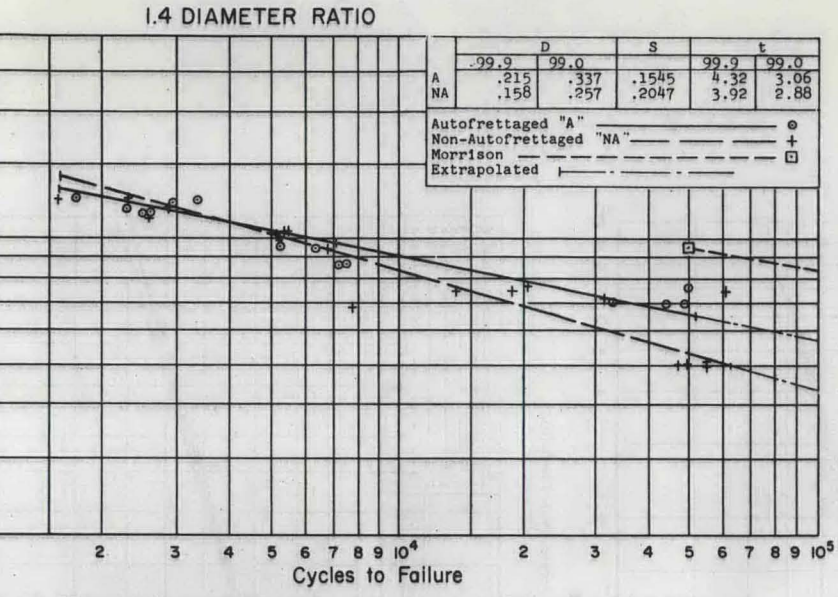

Fig. 9 Difference in principal bore stress versus cycles to failure for 1.4-diameter ratio

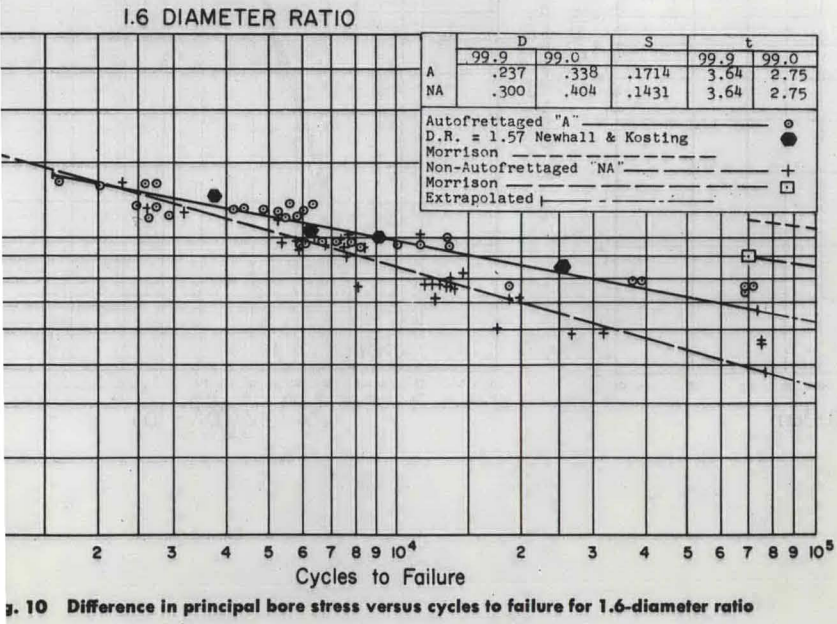

Fig. 10 Difference in principal bore stress versus cycles to failure for 1.6-diameter ratio

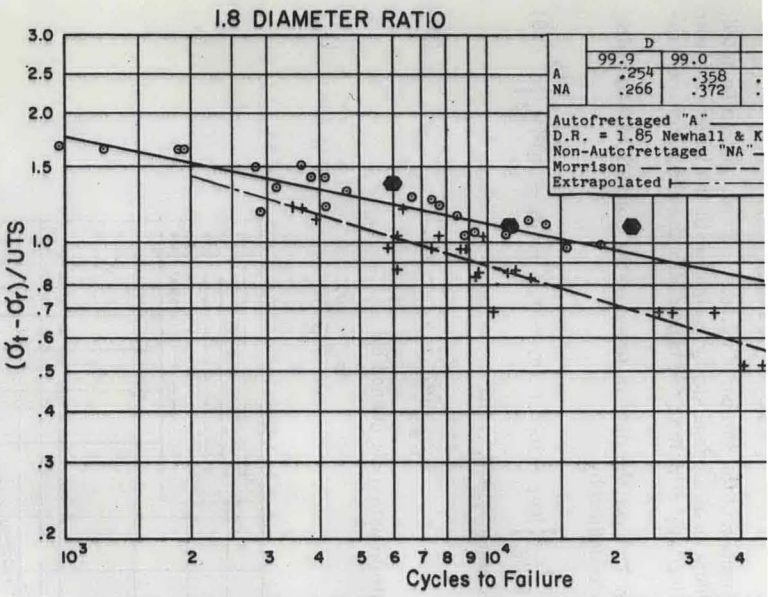

Fig. 11 Difference in principal bore stress versus cycles to failure for 1.8-dia

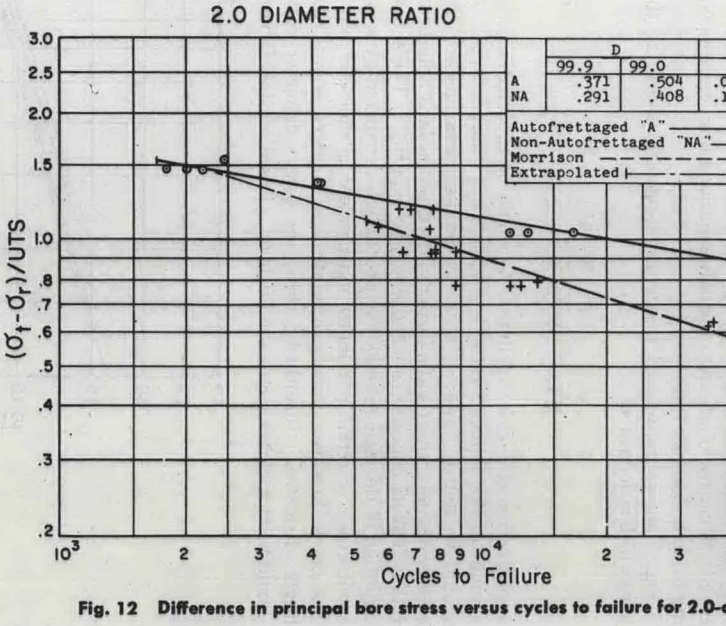

Fig. 12 Difference in principal bore stress versus cycles to failure for 2.0-

may also be used as shown in Fig. 8. It should be noted, however, that again, as in the case of σ_t versus life, as shown in Fig. 5, the smaller diameter ratios lie above the larger diameter ratios.

As can be noted from the similarity of correlation coefficients which are related to the spread of the data for the various cyclic parameters shown in Figs. 5 through 8, it makes little difference statistically as to what cyclic stress or strain parameter is chosen to plot the data. The magnitude of the data spread due to diameter-ratio dependence is approximately the same in each case with only the order being different. For the purpose of this report then, all data, unless otherwise specified, will be presented in terms of the normalized difference in principal bore stress as defined by equation (8).

Effects of Autofrettage on Fatigue Life. The effects of autofrettage on fatigue life, as compared to the nonautofrettaged condition, is shown in Figs. 9, 10, 11, and 12, respectively, for the diameter ratios of 1.4, 1.6, 1.8, and 2.0. A compilation of the least-squares lines for all diameter ratios in terms of the difference in principal bore stresses and cyclic pressure is shown in Figs. 13 and 14, respectively.

In the statistical data shown in the legend of these figures, S is the standard deviation as defined by

$$S = \sqrt{(1 - r^2)\frac{\Sigma(x - \bar{x})^2}{n - 2}} \tag{12}$$

and t_c is the confidence-level coefficient for a two-sided normal distribution which depends on the confidence level and the degrees of freedom defined as the number of test points minus two. In the figures, the values of t shown are for 99.9 percent and 99.0 percent confidence level. Coefficients for other confidence levels can be obtained from standard texts on statistics dealing with the treatment of experimental data [5, 6].

The limits for a given confidence band are closely approximated by the following relationship where $\bar{x}$ is in $\log_{10}$

$$x_c = \bar{x} \pm t_c S \tag{13}$$

which represents a straight line parallel to the least-squares line on the curves presented. The relationship of cycles to failure to x is

$$N = (10^{x_c}) \tag{14}$$

For simplicity in using these curves, the value of D_c shown in the legend is the ratio of cycles to failure for the lower limit of con-

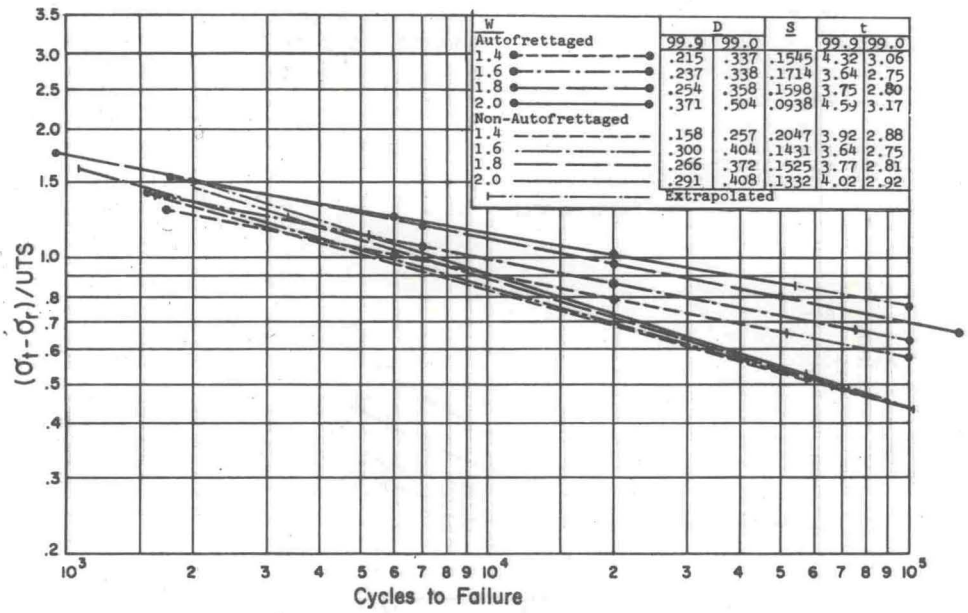

Fig. 13 Difference in principal bore stress versus cycles to failure for 1.4–2.0-diameter ratios

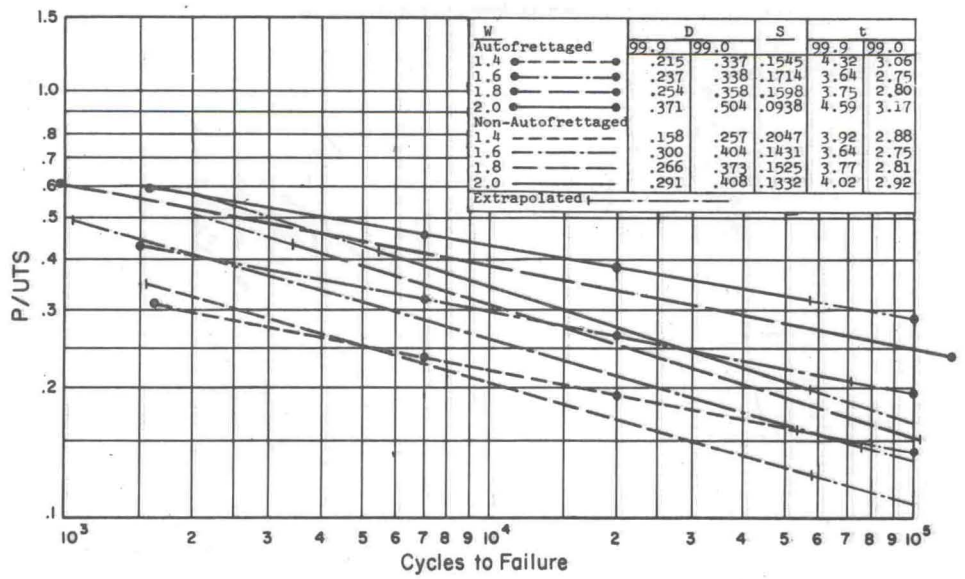

Fig. 14 Pressure versus cycles to failure for 1.4–2.0-diameter ratios

fidence level indicated to the least-squares value at a particular stress or pressure level. Since a two-sided normal distribution curve is assumed, the confidence level associated with the lower limit of the number of cycles to failure alone is increased by half the difference to unity for the values given. For example, the lower limit of life with 99.95 percent confidence is given by the relation

$$N_{99.95} = \overline{N}D_{99.9} \tag{15}$$

As can be seen in the above-mentioned figures, there is an improvement in the fatigue characteristics of autofrettaged cylinders as compared to the nonautofrettaged condition. The relative benefit increases with decreasing operating stress level and increasing diameter ratio. The increase in life of the autofrettaged cylinders over the nonautofrettaged condition for several stress levels is summarized in Fig. 15. For example, considering the case of 2.0-diameter ratio operating at a normalized difference in principal stress of 0.9, which is approximately 10 percent below the elastic breakdown condition, as predicted by the von Mises yield criterion, the increase in life is a factor of 3.6. Proportional benefits are obtained in the allowable operating stresses to cause failure. Considering the same example, as above, for a life of 50,000 cycles, the average operating stress level, as a result of autofrettage, may be increased 50 percent over that for the nonautofrettaged condition.

Fig. 16 is a plot of diameter ratio versus cycles to failure for several differences in principal stress levels. As can be seen, there is a slight diameter-ratio dependency for the nonautofrettaged cylinders which is attributed primarily to the greater distance over which the crack must propagate as the diameter ratio increases, before ductile rupture occurs. It is readily seen, however, that the autofrettaged cylinders exhibit a very substantial diameter-ratio dependency with the benefit from autofrettage increasing with increased diameter ratio. From equation (3) this would be expected since the magnitude of the compressive residual bore stress increases with diameter ratio. In the region of 1.8 to 2.0-diameter ratio, the slope of the diameter ratio versus cycles to failure curve changes for the autofrettaged condition and approaches that characteristic of the nonautofrettaged cylinders. This indicates that the magnitude of the residual stresses is no longer increasing. However, by equating equation (3) to the yield strength of the material in compression, which is usually assumed substantially equal to that in tension, it can be shown that the maximum residual stress is obtained at a diameter ratio of 2.2, based on the Tresca yield criterion. To some extent, this early change in slope is attributed to the Bauschinger effect which, from associated work that will be reported at a later date, appears to occur at the 2.0-diameter ratio or less for the 100 percent overstrain condition. The Bauschinger effect results in a lowering of the compressive yield strength which, in the case of an

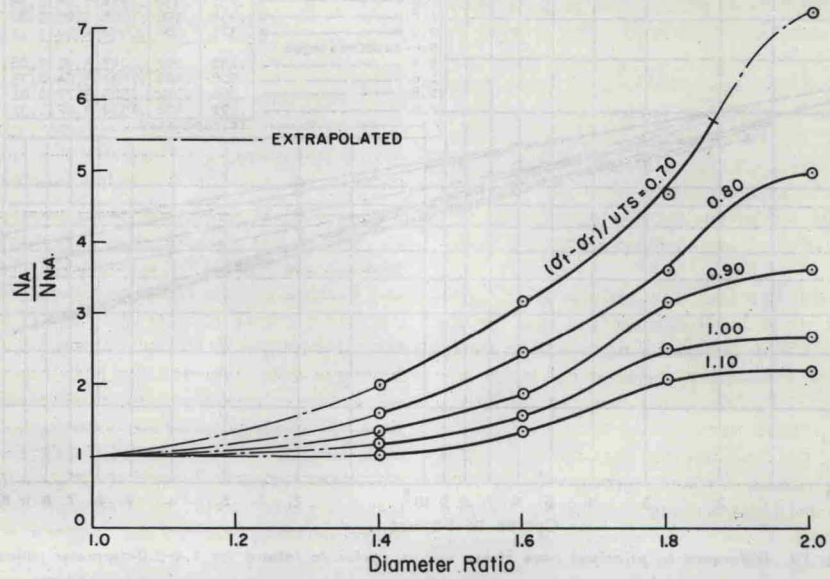

Fig. 15 Ratio of autofrettaged to nonautofrettaged cycles to failure versus diameter ratio

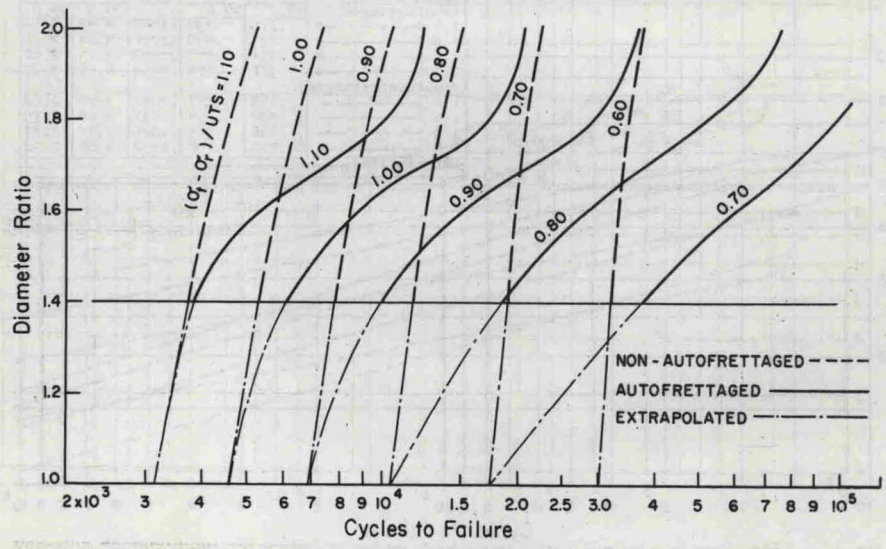

Fig. 16 Diameter ratio versus cycles to failure at various differences in principal bore stress levels

overstrained thick-walled cylinder, limits the maximum level of the compressive residual bore stress beyond which the cylinder will yield in compression. Beyond the 2.0-diameter ratio then, it is anticipated that the slope of the autofrettaged curve will be the same as that for the nonautofrettaged condition.

The study of the fatigue characteristics of thick-walled cylinders directly, as in the manner described herein, has several experimental difficulties, the most significant being attrition of equipment. It would be desirable then to be able to predict the fatigue characteristics of thick-walled cylinders from some simplified fatigue test. One possible approach to this problem will now be discussed.

As the diameter ratio approaches 1, the radial component of the stress approaches 0 with only the tangential stress remaining. As shown in Fig. 16, the autofrettaged also approaches the nonautofrettaged condition as the diameter ratio decreases with convergence at $W = 1$. Since there is only one principal stress at the hypothetical case of $W = 1$, then it may be possible to correlate this condition with a uniaxial tensile-fatigue test. To a first approximation, the slopes of the diameter ratio versus cycles to failure curves for the nonautofrettaged condition are reasonably independent of stress level. Therefore, to determine the fatigue characteristics of thick-walled cylinders of a given material over a wide range of stress levels and diameter ratios would require only the running of a series of tensile-fatigue tests at different stress levels and to determine the slope, only one group of cylinders at a given diameter ratio and stress level. The slope of the diameter ratio versus cycles to failure curves is dependent upon cyclic-stress level for the autofrettaged condition. Consequently, two groups of thick-walled cylinders at widely different stress levels in conjunction with the tensile-fatigue data would be required to establish, to a close approximation, the entire family of curves for a wide range of diameter ratios and stress conditions of the type shown in Fig. 16 for the open-end condition, i.e., $\sigma_z = 0$. The feasibility of this simplified approach will be investigated further.

As the cyclic-stress level increases, the benefits from autofrettage decrease, and at stress levels approaching that for the overstrain pressure, there is little benefit. This is to be expected since the nonautofrettaged cylinders at these stress levels will actually permanently deform; thus, being autofrettaged to a certain degree on the first pressure cycle.

It should be noted that the least-squares lines shown in all of the figures intersect the ordinate which corresponds to 1000 cycles at a stress value closely approaching that for the 100 percent overstrain condition, i.e.,

$$\frac{\sigma_t - \sigma_r}{\text{UTS}} = \frac{1.08\sigma_y \ln W}{\text{UTS}} \left[\frac{2W^2}{W^2 - 1}\right] \tag{16}$$

where $1.08\sigma_y \ln W$ equals the pressure for 100 percent overstrain (3). If the least-squares line were continued to the one-cycle condition, the stress level would be well in excess of the rupture pressure which, for the material considered herein, is only slightly in excess of the overstrain pressure. Instead of continuing on, however, for the cyclic rates considered in this investigation, there is a leveling off in the very low cycle region and the slope of the curve approaches 0 at stress levels in the neighborhood of that associated with the 100 percent overstrain condition. This very low cycle, high stress region is a subject of current study.

Effect of Thermal Treatment After Autofrettage. It has been found in another current investigation that thermal treating high-strength autofrettaged cylinders at approximately 675 F for a period of time tends to increase the elastic load-carrying capacity. As shown in Fig. 17, thermal treatment, however, has little effect on fatigue characteristics as is indicated by the overlapping of the thermally and nonthermally treated data for autofrettaged cylinders in the 1.4 to 1.8-diameter ratio range. Except for this figure then, the thermally and nonthermally treated results were not considered separately.

Effect of Surface Finish and Tensile-Strength Variations. The internal diameter surface finishes of the specimens utilized in this program varied from approximately 16 to 125 RMS as measured along the longitudinal axis. However, analysis of the data does not indicate any trends toward dependency of the results upon surface finish over the range encountered.

The fatigue characteristics similarly appear to be proportional to the tensile-strength level for the range of ultimate tensile strength from 160,000 to 190,000 pounds per square inch.

Comparison of Results With Other Investigations. In Figs. 9, 10, 11, and 12, the data of other investigators, Morrison [1], and Newhall and Kosting [2], are included. In the case of the Newhall and Kosting data for large open-end cylinders at ultimate tensile-strength levels of 115,000 and 154,000 pounds per square inch, the correlation with the data presented herein is excellent. The Morrison data, however, for both the autofrettaged and nonautofrettaged condition, lies substantially above the presented data. In discussing this apparent discrepancy one must consider that there are three substantial differences in the experimental conditions between the two investigations. Whereas Morrison's specimens were tested as closed-end cylinders, the results presented herein considered the open-end condition, i.e., the longi-

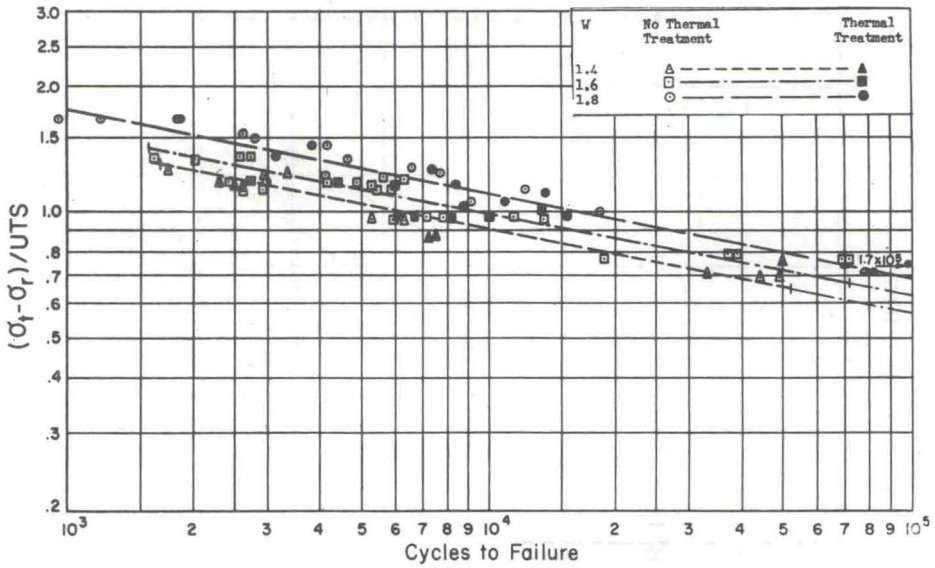

Fig. 17 Differences in principal bore stress versus cycles to failure for autofrettaged cylinders showing the effect of thermal treatment

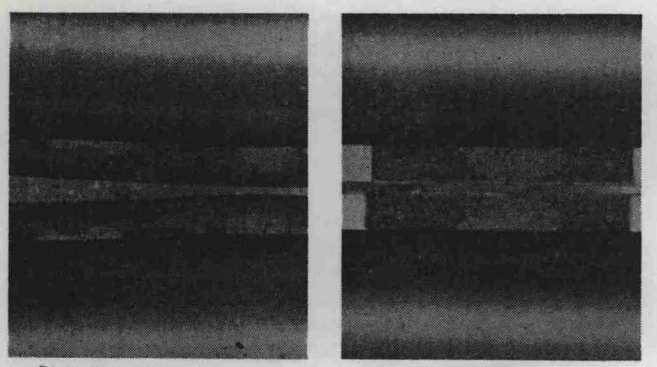

Diameter ratio = 1.4
Test pressure = 50,000 psi
Cycles to failure = 3380

Diameter ratio = 1.4
Test pressure = 30,000 psi
Cycles to failure = 31,300

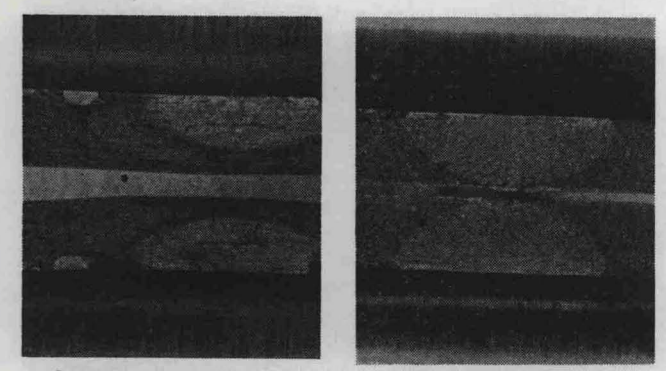

Diameter ratio = 1.8
Test pressure = 70,000 psi
Cycles to failure = 2880

Diameter ratio = 1.8
Test pressure = 30,000 psi
Cycles to failure = 40,300

Fig. 18 Typical fatigue fractures

tudinal stress is effectively zero. If the third stress is taken into account theoretically by the octahedral stress parameter, equation (9), the variation is slightly reduced. Except by test, one cannot be certain of the magnitude of the effect of this third stress on fatigue. Therefore, the magnitude by which the third principal stress associated with the closed-end condition affects fatigue is the subject of a current investigation. Second, Morrison used a cyclic pressure rate of approximately 1000 cycles per minute as compared to 6 per minute for this investigation. Third, the bore of Morrison's specimens were lapped to a finish of approximately 1 to 4 RMS as compared to 16 to 125 RMS which could have a pronounced effect in terms of crack initiation. It is difficult to ascertain the magnitude of the contribution of these various differences to the higher fatigue characteristics reported by Morrison. It is most likely, however, that the most important factor is the difference in surface finish. It is interesting to note that the discrepancy is substantially smaller in the case of the autofrettaged data as compared to the nonautofrettaged condition. This is probably due in part to the tendency for the high compressive tangential residual stress to reduce the effectiveness of the rougher bore surface in enhancing crack initiation.

Fracture Analysis. Representative fatigue failures for thick-walled cylinders of 1.4 and 1.8-diameter ratio at low-cyclic and high-cyclic stress levels are shown in Fig. 18. As can be noted, there are two characteristic zones. The first zone, which appears lighter, has a smooth appearance with conchoidal markings. This zone, sometimes called the zone of decohesion [6], is characteristic of a cyclically propagating fatigue crack. The second and remaining zone has a fibrous texture which is characteristic of static rupture in a ductile thick-walled cylinder.

From a macroscopic standpoint, the fatigue crack evidently propagates to the depth at which the remaining material is no longer able to withstand the internal pressure, and ductile rupture occurs. As would be expected then, there should be a correlation between the cyclic stress and the fatigue fracture area and depth. By examining a large number of fracture surfaces of the specimens associated with this study, it has been found that there is an approximate linear relationship between the cyclic-stress parameter and the crack depth divided by the wall thickness as shown in Fig. 19. There is, of course, scatter due to the experimental difficulty of determining the exact location of the boundary between the fatigue crack and fibrous rupture zone, as well as the statistical nature of fatigue data. However, the scatter is not so great that the linear correlation cannot be readily detected over a wide range of cyclic-stress levels and wall ratios. A similar linear relationship also exists for the cyclic-stress parameter versus the crack area divided by the square of the wall thickness.

It should be noted that only the fatigue crack causing final failure was considered in the above plots. Smaller cracks were also noted in several other areas of the specimen. An example of this condition is shown in Fig. 18, where several smaller fatigue cracks are readily visible.

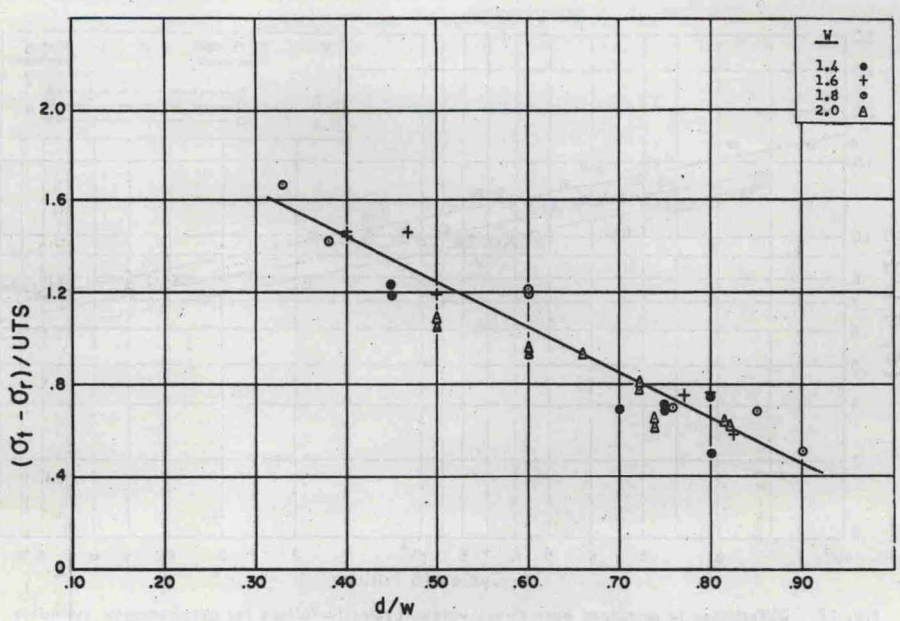

Fig. 19 Difference in principal bore stress versus crack depth/thickness

Conclusions

Data for the hydrostatic fatigue characteristics of high-strength thick-walled cylinders in the range of 10^3 to 10^5 cycles to failure are presented. Based on this investigation, the following points have been established.

1 Autofrettage significantly improves the fatigue characteristics of thick-walled cylinders at stress levels lower than those associated with the overstrain pressure. The degree of improvement increases as the cyclic stress level decreases.

2 Using the difference in principal bore stress as the cyclic parameter, the fatigue characteristics improve with increasing diameter ratio. This increase with diameter ratio is small in the case of the nonautofrettaged condition. In the case of autofrettaged cylinders, the increase in fatigue life with diameter ratio is substantial. The rate of improvement in the autofrettaged cylinders approaches that for the nonautofrettaged condition beyond a diameter ratio of 2.0.

3 The slope of the difference in principal bore stress versus cycles to failure curve appears to approach zero below 10^3 cycles to failure.

4 Based on the similarity in the correlation coefficient, no single cyclic stress or strain parameter evaluated for the presentation of thick-walled cylinder fatigue data offered significant advantage over the others.

5 Thermal treatment of the overstrained cylinders at 675 F for 6 hours did not affect fatigue characteristics.

6 There is a correlation between the cyclic-stress level and the area and depth of the fatigue crack to the point of ductile rupture; the depth of the crack decreasing with increasing stress level.

7 Internal-diameter surface finishes varying from 16 to 125 micro-inches RMS did not show a consistent pattern in affecting the fatigue life.

8 The fatigue characteristics appear to be proportional to the tensile-strength level for the range of ultimate tensile strength from 160,000 to 190,000 pounds per square inch.

Acknowledgment

The authors wish to thank the following individuals who have helped bring this investigation to the current stage: Mr. R. A. Petell and his staff for the conduct of the experimental work, Mr. D. P. Kendall for his helpful discussions, Mr. P. Loatman for the statistical analysis of the experimental data, Mr. Earl Skelton for his help with the data and statistics, and Dr. R. E. Weigle and Mr. M. Pascual for their constructive comments.

References

1 Morrison, Crossland, and Parry, "The Strength of Thick Cylinders Subjected to Repeated Internal Pressure," JOURNAL OF ENGINEERING FOR INDUSTRY, TRANS. ASME, Series B, vol. 82, 1960, pp. 143–153.

2 D. H. Newhall and P. R. Kosting, "Progressive Stress Damage and Strength of Centrifugally Cast CW Gun Tubes," 1949, Watertown Arsenal Laboratory, 731/281.

3 T. E. Davidson, C. S. Barton, A. N. Reiner, and D. P. Kendall, "The Autofrettage Principle as Applied to High-Strength Light-Weight Gun Tubes," Technical Report WVT-RI-5907, Revision 1, Watervliet Arsenal, Watervliet, N. Y.

4 H. Sigwart, "Influence of Residual Stresses on the Fatigue Limit," Fig. 3.41, page 273, of the Proceedings of the International Conference on Fatigue of Metals, 1956, published by The Institution of Mechanical Engineers.

5 Sines and Waisman, "Metal Fatigue," McGraw-Hill Book Company, Inc., New York, N. Y., 1959, pp. 112–141.

6 R. A. Fisher and F. Yates, Oliver, and Boyd, "Statistical Tables for Biological, Agricultural, and Medical Research," Table III.

7 Crussard, Plateau, Tamhankar, Henry, and Lajeunesse, "A Comparison of Ductile and Fatigue Fractures," "Fracture," J. Wiley & Sons, Inc., New York, N. Y., 1960, p. 593.

Printed in U. S. A.